Applied Catalysis B: Environmental 90 (2009) 618–627

Contents lists available at ScienceDirect

Applied Catalysis B: Environmental

journal homepage: www.elsevier.com/locate/apcatb

# The effect of Fe/Cu ratio in the synthesis of mixed Fe,Cu,Al-clays used as catalysts in phenol peroxide oxidation

M.N. Timofeeva [a,*], S.Ts. Khankhasaeva [b], E.P. Talsi [a,c], V.N. Panchenko [a], A.V. Golovin [c], E.Ts. Dashinamzhilova [b], S.V. Tsybulya [a,c]

[a] Boreskov Institute of Catalysis SB RAS, Prospekt Akad. Lavrentieva 5, 630090, Novosibirsk, Russian Federation, Russia
[b] Baikal Institute of Nature Management SB RAS, Ulan-Ude, Str. Sakh'yanova 8, 670047, Ulan-Ude, Russian Federation, Russia
[c] Novosibirsk State University, Prospekt Akad. Koptyuga 2, Novosibirsk 630090, Russian Federation, Russia

ARTICLE INFO

*Article history:*
Received 2 February 2009
Received in revised form 21 April 2009
Accepted 25 April 2009
Available online 3 May 2009

*Keywords:*
Pillared clays
Effect of synthesis parameters
Hydrogen peroxide
Phenol
Oxidation
EPR

ABSTRACT

Mixed Fe,Cu,Al-clays (Fe,Cu,Al-MM) were prepared from Ca-montmorillonite (Mukhortala, Buryatia) at OH/(Fe + Cu + Al) 2.4 and Al/(Fe + Cu) 10/1. Effect of Fe/Cu ratio of Fe,Cu,Al-containing pillaring solution on structural properties of Fe,Cu,Al-MM was examined. Characterization studies were performed by use of XRD, FTIR, DR-UV–vis and $N_2$-adsorption/desorption analysis. The increase in copper loading leads to the decrease in total surface area, micropore volume and interlay distance of Fe,Cu,Al-MMs. It was found that the decrease in Fe/Cu ratio is favourable for the formation of oligomeric iron species. The relationships between preparation conditions, iron state, catalytic activity and stability to leaching were revealed in wet phenol oxidation with $H_2O_2$. The introduction of copper ions results in catalytic reaction acceleration that was interpreted in terms of the increase of radical generation rate.



## 1. Introduction

Nowadays, an investigation of catalysts, which would have a high activity for oxidation of toxic organic pollutants, such as phenol, substituted phenols and dyes, in aqueous solutions under mild conditions, is the objective of many scientists and engineers working in the wastewater treatment field. One of the promising catalysts for organic pollutants oxidation is layered clays intercalated by polymeric metal-containing inorganic oxocations due to the high material's resistance and stability, the development of microporosity, the great surface area and the presence of acid sites (Brönsted and Lewis sites) [1–4]. Nowadays the main cations used for the intercalation of clays are so-called Keggin type $[Al_{13}O_4(OH)_{24}(H_2O)_{12}]^{7+}$ cation ($Al_{13}^{7+}$) and metal-substituted $Al_{13}^{7+}$ cations with the nominal composition $Fe_xAl_y^{n+}$ [4–8]. Fe,Al-pillared clays (Fe,Al-PILCs) allow carrying out hydroperoxide organic pollutants oxidation at pH 6.0–6.2 [9,10]. Considerable body of work have been reported on the synthesis of Fe,Al-PILCs [4–10]. It was demonstrated that the main properties of Fe,Al-PILCs, such as textural, structural and catalytic properties, depend on the method of introduction of $Fe_xAl_y^{n+}$ in the layered clay, the degree of isomorphous substitution, the chemical composition and crystallinity of layered clay, structure and composition of $Fe_xAl_y^{n+}$ cation in pillaring solution. Thus, the nature of pillaring agent (mixed $Fe_xAl_y^{n+}$) strongly depends on OH/(Al + Fe) and Al/Fe ratios [6,8,10]. It was found that the higher Al/Fe and OH/(Al + Fe) ratios favour the increase in the formation of $FeAl_{12}^{7+}$ polyoxocation. It worth noting, that the maximum interlayer distance in Fe,Al-PILC can be obtained when the Keggin type $Al_{13}^{7+}$ cation is present in a pillaring solution [11]. The prolonged aging time of Fe,Al-containing pillaring solution (Al/Fe = 10/1 and OH/(Al + Fe) = 2.4) is beneficial to the increase in the total surface area, total pore-volume and micropore volume in Fe,Al-PILCs due to the transformation of $Al_{13}^{7+}$ into $Al_{24}O_{72}$ ($Al_{13}$ dimer) and other polynuclear cations [12,13]. According to [10], the higher value of surface area and higher content of micropore were observed in Fe,Al-PILC samples after modification of Na-clay by Fe,Al-solution (Al/Fe = 10/1 and OH/(Al + Fe) = 2.4) aged for >7 days. Variation of Al/Fe, OH/(Fe + Al) ratio and aging time of Fe,Al-containing pillaring solution permits the adjustment of the oligomeric iron oxide clusters content. The larger OH/(Fe + Al) ratio, the smaller content of oligomeric iron species. Isolated iron species dominate at OH/(Fe + Al) = 2.4. The Al/Fe ratio and calcination temperature affect the state of the iron species in the Fe,Al-PILCs. The increase in Al/Fe ratio and calcination temperature from 400 to 500 °C leads to the increase in the formation of isolated iron species. According to [10], the increase in calcination temperature and/or aging time of Fe,Al-pillaring solution is favourable to decrease in the iron

* Corresponding author. Tel.: +7 383 330 72 84; fax: +7 383 330 50 86.
*E-mail address:* timofeeva@catalysis.ru (M.N. Timofeeva).

0926-3373/$ – see front matter © 2009 Elsevier B.V. All rights reserved.
doi:10.1016/j.apcatb.2009.04.024

leaching and an increase in the reaction rate of phenol oxidation with $H_2O_2$ due to the formation of isolated iron species.

Unfortunately, for the heterogeneous Fenton type catalytic system ($Fe^{II}$–$Fe^{III}/H_2O_2$), the reaction starts after an induction period, which depends on iron state in the solids ($Fe^{II}$–$Fe^{III}$), radical generation rate and etc. The increase of temperature and/or pH reaction medium permits the decrease of induction period. For Fenton's systems, the induction period typically decreases with increasing acidity of the phenol solution to pH 2.5–4.0 due to the rise of $H_2O_2$ decomposition rate. However, the increase of an acidity of the phenol solution can be accompanied with substantial iron leaching. One can assume that the induction period can be decreased by either variation of surface acidity or introduction of multimetal-containing cation in the layered clay which allows the increase of radical generation rate. For example, combinations of three elements have been used for preparation of La,Ca,Al-PILCs [14], Sm,Mn,Al-PILCs [15] and Al,Ce,$M^{II}$-PILCs ($M^{II}$ - divalent cation of $Co^{2+}$, $Ni^{2+}$, $Zn^{2+}$ or $Mg^{2+}$) [16]. The mixed pillared clays were prepared by (a) using partially hydrolyzed threemetal-containing pillaring solutions; (b) using mixture of two partially hydrolyzed $M^{III}$/Al and $M^{II}$/Al pillaring solutions; (c) adsorption of divalent cation on bisubstituted $M^{III}$,Al-PILCs; and (d) the isomorphous substitution of alumina in $M^{III}$,Al-PILCs by transition metal. These $M^{III}$,$M^{II}$,Al-pillared clays possessed higher thermal stabilities than the monosubstituted and bisubstituted ones. Moreover the basal spacing and specific surface area of these solids were 15–20 Å and 49–219 $m^2$/g, respectively.

According to [17] clay can be successfully pillared with solutions of Al,Fe- or Al,Ce,Fe-polyhydroxocations. These systems were highly efficient for hydroperoxide phenol oxidation in very mild conditions (298 K, pH 3.7 and atmospheric pressure). The addition of Ce in PILC favours the increase of catalytic activity of such systems. Recently, Fe,$M^{II}$,Al-PILCs ($M^{II}$–$Mn^{2+}$, $Co^{2+}$, $Ni^{2+}$, $Cu^{2+}$, $Zn^{2+}$) were prepared by the isomorphous substitution of alumina in Fe,Al-PILC by transition metal and used as catalysts for wet phenol oxidation with $H_2O_2$ under mild reaction conditions [18]. It was demonstrated that Fe,$M^{II}$,Al-PILCs are good oxidation catalysts due to the variation of Brónsted acidity. Moreover the induction period was reduced by the addition of the third transition metal in Fe,Al-PILCs [19]. It is well-known that Cu,Al-PILCs are active catalysts for the oxidation of different organic compounds [20–24]. It was established that the copper content and the procedure of Cu,Al-PILCs preparation significantly influence on their catalytic activity in phenol oxidation with hydrogen peroxide [22,25]. Catalytic activity increases with the increase of Cu content in Cu,Al-PILCs. It is remarkable that, induction period was absent in reactions of PhOH and dyes oxidation [19,22,25].

The aim of this study was to developed a simple method for preparation of mixed Fe,Cu,Al-containing clay (Fe,Cu,Al-MM) from natural layered aluminosilicate containing 90–95% montmorillonite by exchanging interlayer ions to polyoxocations. The nature of polyoxocations was varied by using (a) partially hydrolyzed Fe,Cu,Al-containing pillaring solutions; and (b) mixture of two partially hydrolyzed Fe/Al and Cu/Al pillaring solutions. The effect of the Fe/Cu ratio of Fe,Cu,Al-containing pillaring solution on structural properties of Fe,Cu,Al-MMs was examined. The catalytic properties of Fe,Cu,Al-MMs were assessed in full phenol oxidation with $H_2O_2$. The relationships between preparation conditions, iron and copper state, catalytic activity and stability to leaching were revealed.

## 2. Experimental

### 2.1. Materials

The natural layered aluminosilicate (MM) was obtained from a bed located in Mukhortala, Buryatia. The mineral contains 90–95% of a calcium-rich montmorillonite with the total chemical composition: $SiO_2$ – 65.50; $Al_2O_3$ – 17.10; $Na_2O$ – 0.16; $K_2O$ – 0.17; MgO – 1.36; CaO – 1.06; ZnO – 0.018; MnO – 0.002; $Fe_2O_3$ – 1.07; CuO – 0.002; $H_2O$ – 13.56. The cation exchange capacity ($Ca^{2+}$, $Mg^{2+}$, $K^+$ and $Na^+$) was 0.7 meq/g of (ignited) clay.

### 2.2. Synthesis of Fe,Cu,Al-containing clays

#### 2.2.1. Cu,Al-MM

Cu,Al-MM was prepared following a procedure described in [22]. The Cu,Al-pillaring solution (Al/Cu = 10/1) was prepared from mixing 0.1 M $AlCl_3$ and 0.1 M $CuCl_2$ with following hydrolysis using 1 M NaOH solution (OH/(Al + Cu) = 2.0), then Cu,Al-mixture was held at room temperature for 14 days and 36 h at 90 °C. Cu,Al-solution was added to the clay (solution/clay = 3 mM Cu/g and solid/liquid = 1/100 g/g) at room temperature and the mixture was held at room temperature for 1 day. The intercalated clay was filtered by suction, washed with distilled water, dried in air and calcinated at 500 °C for 2 h. The conditions of preparation and chemical composition of this solid are reported in Table 1.

#### 2.2.2. Fe,Cu,Al-MMs

Fe,Cu,Al-MMs were synthesized by two routes. Method 1: The Fe,Cu,Al-pillaring solution (Al/(Fe + Cu) = 10/1) was prepared from mixing 0.2 M $AlCl_3$, 0.1 M $CuCl_2$ and 0.1 M $FeCl_3$ with following hydrolysis using 1 M NaOH solution (OH/(Fe + Cu + Al) = 2.4), then mixture was held at room temperature for 14 days. Three ratios Fe/Cu, namely 0.3/0.7, 0.5/0.5 and 0.7/0.3, were considered. Solution of Al/(Fe + Cu) was added to the clay at room temperature and the mixture was held at room temperature for 1 day. The intercalated clay was filtered by suction, washed with distilled water, dried in air and calcinated at 500 °C for 2 h. **Method 2**: Pillaring solution was prepared by mixing of Al/Fe (5/0.5) and Al/Cu (5/0.5) solutions hydrolyzed by 1 M NaOH solution (OH/(Fe + Al) = 2.4 and OH/(Cu + Al) = 2.0). The designation of the samples and the main conditions of these syntheses are given in Table 1.

#### 2.2.3. Synthesis of Fe,Al-MM

Synthesis of Fe,Al-MM was performed using a procedure described in [10]. The Fe,Al-pillaring solution (Al/Fe = 10/1) was prepared from mixing 0.2 M $AlCl_3$ and 0.1 M $FeCl_3$ with following hydrolysis using 1 M NaOH solution (OH/(Al + Fe) = 2.4), then Fe,Al-mixture was held at room temperature for 14 days. Fe,Al-solution was added to the clay at room temperature and the mixture was held at room temperature for 1 day. The intercalated clay was filtered by suction, washed with distilled water, dried in air and calcinated at 500 °C for 2 h. The conditions of preparation and chemical composition of this solid are reported in Table 1.

### 2.3. Instrumental measurements

The porous structure of the supports was determined from the adsorption–desorption isotherm of $N_2$ (77 K) on a SORBI-M equipment. The specific surface area ($S_{BET}$) was calculated by the Brunauer–Emmett–Teller (BET) method. The X-ray diffraction patterns were measured on a X-ray diffractometer XTRA (Thermo-ARL) with Cu-$K_\alpha$ ($\lambda$ = 1.5418 Å) radiation.

The DR-UV–vis spectra were recorded on a UV-2501 PC Shimadzu spectrometer with a IRS-250A accessory in the 190–900 nm range with a resolution of 2 nm. $BaSO_4$ was used as standard. The samples in a form of powders were placed into a special cell for DR-UV–vis measurement. Infrared spectra were recorded on a BOMEM-MB-102 spectrometer in 4000–250 $cm^{-1}$ range with a resolution of 4 $cm^{-1}$ (compressed pellets of 2 mg of catalysts and 500 mg KBr). EPR spectra on a Bruker ER-200D

**Table 1**
Specification of Fe,Cu,Al-MM samples.

| | Designation of sample | Conditions of synthesis[a] (mol/mol/mol) | | | Chemical composition of product, (wt.%) | | |
|---|---|---|---|---|---|---|---|
| | | Fe | Cu | Al | Fe | Cu | Al |
| 1 | Natural clay | – | – | – | 0.8 ± 0.2 | <0.01 | 8.9 ± 0.1 |
| 2 | Cu,Al-MM | 0.0 | 1.0 | 10.0 | 0.2 ± 0.1 | 0.70 ± 0.1 | 14.0 ± 0.1 |
| 3 | Fe,Cu,Al-MM(0.3/0.7) | 0.3 | 0.7 | 10.0 | 1.0 ± 0.1 | 0.05 ± 0.01 | 12.8 ± 0.1 |
| 4 | Fe,Cu,Al-MM(0.5/0.5) | 0.5 | 0.5 | 10.0 | 1.3 ± 0.1 | 0.06 ± 0.01 | 10.9 ± 0.1 |
| 5 | Fe,Cu,Al-MM(0.7/0.3) | 0.7 | 0.3 | 10.0 | 1.5 ± 0.1 | 0.06 ± 0.01 | 10.9 ± 0.1 |
| 6 | Fe,Al-MM | 1.0 | 0.0 | 10.0 | 1.7 ± 0.1 | <0.01 | 13.8 ± 0.1 |
| 7 | Fe,Cu,Al-MM(0.5/0.5)$_m$[b] | 0.5 | 0.5 | 10.0 | 1.8 ± 0.1 | 0.17 ± 0.01 | 12.8 ± 0.1 |

[a] (OH/(Al + Fe + Cu)) = 2.4.
[b] Pillaring solution was prepared by mixing of Fe/Al (0.5/5) and Cu/Al (0.5/5) solutions.

spectrometer at 9.3 GHz, modulation frequency 100 kHz, modulation amplitude 2 G.

### 2.4. Catalytic tests

The phenol oxidation was carried out at 50 °C in a glass thermostated vessel equipped with a stirrer and a reflux condenser. The reactor was charged with a mixture of PhOH/$H_2O_2$ (30 wt.% in water) = 1:14 mol mol$^{-1}$ (20 ml of 10 mM phenol solution in water) and a catalyst (typically, 1.0 g L$^{-1}$). The phenol concentration in the solution was determined using UV–vis (Specord UV–vis M-40 instrument, λ = 273 nm, accuracy ±10%). The TOC concentration was determined by the Shimadzu TOC analyzer.

The iron content in samples was determined by means of the following procedure. The iron was transformed into solution in the form of $Fe^{3+}$ iron by boiling sample in $HNO_3$–HCl mixture and then it was allowed to react with 1,10-phenanthroline. The absorbance of the iron–phenanthroline complex was measured by UV–vis at λ = 510 nm. The copper content in Fe,Cu,Al-MMs was determined by atomic absorptive analysis (AAS Solaar M 6 spectrometer).

The aluminium content in samples was determined by means of the following procedure. The aluminium was transformed into solution in the form of $Al^{3+}$ iron by fusing of sample with $Na_2B_4O_7$–$Na_2CO_3$–$KNO_3$ mixture and then it was dissolved in HCl (HCl:$H_2O$ 1:3 vol/vol). This solution obtained was allowed to react with aurintricarboxylic acid. The absorbance of the aluminium–aurintricarboxylic acid complex was measured by UV–vis at λ = 520 nm.

### 2.5. Adsorption tests

PhOH adsorption onto Fe,Cu,Al-MMs was studied in a glass thermostated reactor under stirring at 50 °C.The reactor was loaded with 100 mg Fe,Cu,Al-MM and 20 ml of a PhOH aqueous solution (10 mM). At regular time intervals, aliquots were taken and the phenol concentration was determined by UV–vis at λ = 273 nm.

The monoazo dye acid chrome dark-blue ($C_{16}H_9O_9Na_2ClS_2N_2$, ACDB) adsorption onto Fe,Cu,Al-MMs was studied in a glass thermostated reactor under stirring at 50 °C. The reactor was loaded with 20 mg Fe,Cu,Al-MM and 20 ml of a ACDB aqueous solution (0.1 mM). At regular time intervals, aliquots were taken and the ACDB concentration was determined by UV–vis at λ = 510 nm [10].

### 2.6. Spin trap experiments

2,2,6,6-Tetramethylpiperidine (TEMP) was obtained from Aldrich. Electron paramagnetic resonance (EPR) spin trapping of the radical oxygen species formed during the catalytic wet oxidation was performed using a Bruker ER-200D spectrometer at room temperature using a flat quartz cell which is typically used to perform EPR measurements in polar solvents. Spin trap experiments were carried out by adding 0.58 mmol of $H_2O_2$ to a mixture, containing 0.2 mmol of PhOH, 20 mg of Fe,Al-MM (or Fe,Cu,Al-MM) and the spin trap (0.25 mmol of TEMP) in 5 ml $H_2O$.

## 3. Results

### 3.1. Effect of synthesis parameters on structural and textural properties of Fe,Cu,Al-MMs

Fe,Cu,Al-MM samples have been synthesized at OH/(Fe + Cu + Al) 2.4 and Al/(Fe + Cu) 10/1 (Table 1). Tables 1 and 2 summarize the results of the chemical analysis, main textural characteristics and basal spacing ($d_{0\,0\,1}$) of Fe,Cu,Al-MMs. The elemental analysis indicates that the starting natural layered aluminosilicate was effectively modified in its chemical composition (Table 1). A tendency to increase of the Fe content is verified as its content increases in the Fe,Cu,Al-pillaring solution. Note that the Fe content increases in Fe,Cu,Al-MM, while that of Cu remains practically constant. This phenomenon may be explained by the change in the iron and copper state with changing Fe/Cu ratio in pillaring solution. According to $^{27}$Al NMR spectroscopic data, the $Al_{13}^{7+}$ cation is present in all of Fe,Cu,Al-pillaring solutions (Fig. 1). Two signals were observed in the spectra of solutions prepared at Al/Fe 10/1 and Al/Cu 10/1. The first signal at 0 ppm is assigned to monomeric Al species [26,27]. The second signal at 62.5 ppm is attributed to Al atoms in four-fold coordination within a polymeric structure of $Al_{13}^{7+}$ complex [26,28,29]. The addition of $Cu^{2+}$ into pillaring solution leads to the disappearance of a signal at 0 ppm, which is likely the result of interaction between $Al^{3+}$ and products of hydrolysis of $FeCl_3$ and $CuCl_2$, such as $Fe(OH)_2^+$ and/or $Fe_2(OH)_4^{2+}$, $[Cu_2(OH)_3]^+$, mixed units $[M^{2+}_{1-x}M_x^{3+}]^{z+}$ ($[Cu_4Al_2(OH)_{12}]^+$ and etc.

The IR spectra of the natural layered aluminosilicate (MM) and Fe,Cu,Al-MMs are presented in Fig. 2. Bands at 1090 and 1047 cm$^{-1}$ assigned to stretching vibrations of silica-oxygen tetrahedrons $\nu_{as}$(Si–O–Si) and band at 471 cm$^{-1}$ assigned to the bending $\delta$(Si–O) and stretching $\nu$(M–O) vibrations [30,31] were observed in IR spectrum of natural layered aluminosilicate. These bands are appreciably shifted in IR-spectra of Fe,Cu,Al-MMs. Moreover, the intensities of a band of deformation of $Al_2OH$ at 918 cm$^{-1}$ and bands at 624 and 527 cm$^{-1}$ ($\delta$(Si–O), $\nu$(M–O) [32–34] and Si–O–Al (octahedral Al) [35]) decrease with increase of Fe/Cu ratio in pillaring solution. At the same time spectra of Fe,Cu,Al-MMs exhibit the $Fe_2OH$ band at 825 cm$^{-1}$, Fe–O out-of-plane vibration at 660 cm$^{-1}$ and $Al_2OH$ bending bands around 945 cm$^{-1}$ [35]. These combined changes in spectra denote on structural changes in the natural layered aluminosilicate after modification by mixed base-hydrolyzed Fe,Cu,Al-solution.

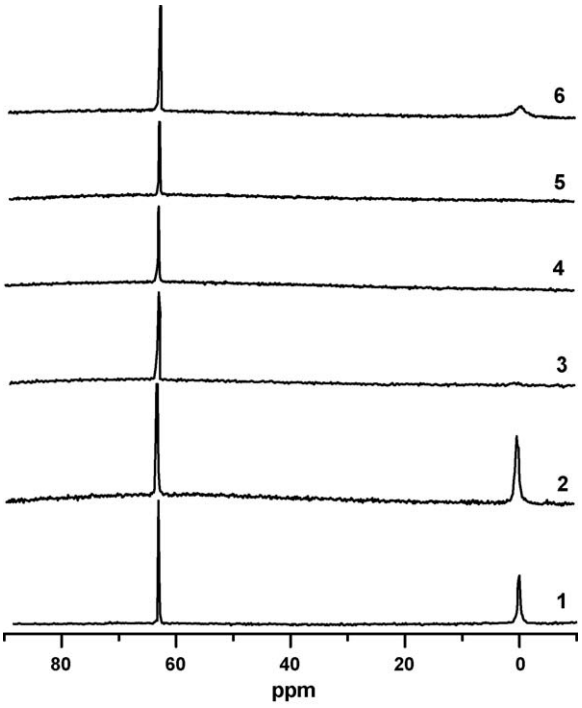


**Fig. 1.** $^{27}$Al NMR spectra of Al-solution prepared at OH/Al = 2.4 (1), and Fe,Al-solutions prepared at OH/(Fe + Cu + Al) = 2.4: Al/Fe/Cu = 10/1/0 (2); Al/Fe/Cu = 10/0.7/0.3 (3); Al/Fe/Cu = 10/0.5/0.5 (4); Al/Fe/Cu = 10/0.3/0.7 (5); Al/Fe/Cu = 10/0/1 (6).

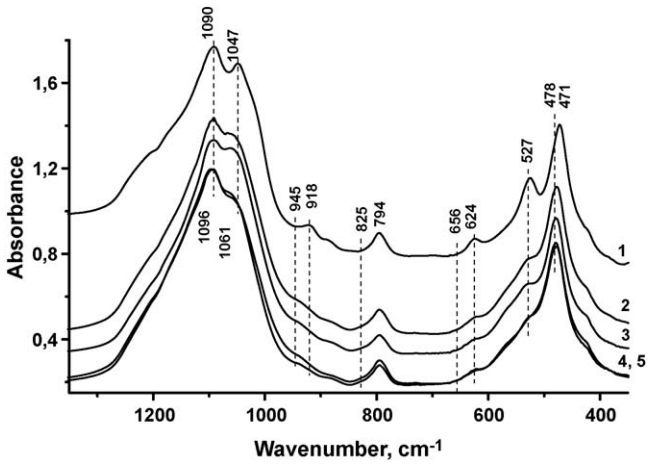


**Fig. 2.** IR spectra of the natural layered aluminosilicate (MM) (1), Cu,Al-MM (2), Fe,Cu,Al-MM(0.3/0.7) (3), Fe,Cu,Al-MM(0.5/0.5) (4), Fe,Cu,Al-MM(0.7/0.3) (5).

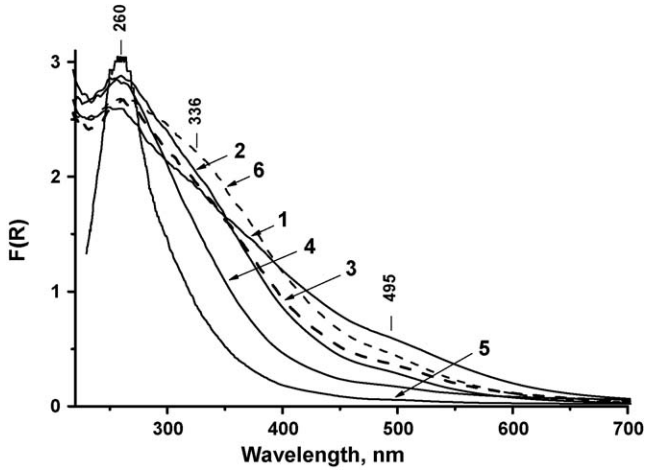


**Fig. 3.** DR-UV–vis spectra of Fe,Cu,Al-MM(0.7/0.3) (1), Fe,Cu,Al-MM(0.5/0.5) (2), Fe,Cu,Al-MM(0.3/0.7) (3), Fe,Al-MM (4), Cu,Al-MM (5), Fe,Cu,Al-MM(0.5/0.5)$_m$ (6).

The state of iron and copper sites of Fe,Cu,Al-MMs was studied by DR-UV–vis spectroscopy. Fig. 3 shows DR-UV–vis spectra for Fe,Cu,Al-MMs synthesized from pillaring solution with different Fe/Cu ratio. As one can be seen from DR-UV–vis data, the state of iron and copper in Fe,Cu,Al-MMs is determined by the Fe/Cu ratio. One band at 260 nm is observed in the spectra of Fe,Al-MM and Cu,Al-MM which is usually assigned both to the $t_1 \rightarrow t_2$ and $t_1 \rightarrow e$ transitions of $Fe^{3+}$ in [$FeO_4$] tetrahedral coordination [36,37]. This band overlaps with band attributed to the charge transfer O → Cu transitions of isolated $Cu^{2+}$ ions in oxygen coordination [38,39], that presents a real challenge for characterization of Fe and Cu state in Fe,Cu,Al-MMs.

The aggregated iron species can be characterized by band at 495 nm [40,41]. The spectrum of Fe,Al-MM shows weak band centered at ~495 nm, indicating that aggregated iron oxide clusters are formed. The intensity of this band was lower in the spectrum of Fe,Al-MM than that in the spectra of Fe,Cu,Al-MMs. Remarkable, that the intensity of this band was higher in the spectrum of Fe,Cu,Al-MM(0.3/0.7) than that in the spectra of Fe,Cu,Al-MM(0.5/0.5) and Fe,Cu,Al-MM(0.7/0.3). Therefore, we can suggest that Fe,Al-MM possesses the larger amount of extra framework iron oligomer and/or aggregated iron oxide clusters than Fe,Cu,Al-MMs. The broad bands in the 300–450 nm region can characterize highly dispersed copper clusters as single-O-bridged copper pairs or double-O-bridged copper pairs (336 nm) [42,43]. The grafting $[Cu(AlO)_n(H_2O)_{6-n}]^{2+}$ species [44,45], which can form if the (AlO) surface groups act as ligands, also show strong absorption in this region. The high intensity of bands in 300–450 nm region points out that Fe,Cu,Al-MMs have larger amount of both isolated and agglomerated copper species, than Cu,Al-MM.

According to XRD data, $d_{001}$ ordering in pillared clays depends on the chemical composition of pillaring solution (Fig. 4). The basal spacing for samples is presented in Table 2. The natural layered aluminosilicate shows 11 Å of basal spacing, but after intercalation of the natural layered aluminosilicate by Cu,Al- and Fe,Al-solutions, basal spacing increases to 18 and 19 Å for Cu,Al-MM and Fe,Al-MM, correspondingly. The addition of Cu ions into

**Table 2**
Structural and textural characteristics of Fe,Cu,Al-MM samples.

| | Sample | $A_{BET}$ ($m^2\ g^{-1}$) | $A_{micro}$ ($m^2\ g^{-1}$) | $\Sigma V_{pore}$ ($cm^3\ g^{-1}$) | $V_\mu$ ($cm^3\ g^{-1}$) | $D_{pore}$ (Å) | $d_{0\,0\,1}$ (Å) |
|---|---|---|---|---|---|---|---|
| 1 | Natural clay | 109 | n.d. | 0.25 | n.d. | 92 | 11 |
| 2 | Cu,Al-MM | 196 | 85 | 0.23 | 0.041 | 35 | 18 |
| 3 | Fe,Cu,Al-MM(0.3/0.7) | 119 | 30 | 0.21 | 0.015 | 43 | 15 |
| 4 | Fe,Cu,Al-MM(0.5/0.5) | 118 | 21 | 0.20 | 0.011 | 69 | 15 |
| 5 | Fe,Cu,Al-MM(0.5/0.5)$_m$[a] | 210 | 86 | 0.25 | 0.042 | 36 | 18 |
| 6 | Fe,Cu,Al-MM(0.7/0.3) | 126 | 27 | 0.22 | 0.014 | 70 | 15 |
| 7 | Fe,Al-MM | 215 | 106 | 0.22 | 0.051 | 41 | 19 |

[a] Pillaring solution was prepared by mixing of Fe/Al (0.5/5) and Cu/Al (0.5/5) solutions.

**Table 3**
Phenol oxidation in the presence of Fe,Cu,Al-MM samples.

| No. | Sample | Condition I[a] | | $\alpha_{PhOH}$[e] (μmol m$^{-2}$) | $\alpha_{ACDB}$[f] (μmol m$^{-2}$) | Condition II[b] | | |
|---|---|---|---|---|---|---|---|---|
| | | TOC removal[c] (%) | Fe leaching[d] (wt.%) | | | $\tau_{20\%}$[g] (min) | $\tau_{100\%}$[g] (min) | Fe leaching[d] (wt.%) |
| 1 | Cu,Al-MM | 30 | <0.1 | 0.87 | 0.076 | 35 | 530 | <0.1 |
| 2 | Fe,Cu,Al-MM(0.3/0.7) | 39 | <0.1 | 1.00 | 0.090 | 37 | 420 | 6 |
| 3 | Fe,Cu,Al-MM(0.5/0.5) | 40 | <0.1 | 0.85 | 0.085 | 35 | 415 | 15 |
| 4 | Fe,Cu,Al-MM(0.7/0.3) | 52 | <0.1 | 0.79 | 0.079 | 40 | 360 | 10 |
| 5 | Fe,Al-MM | 48 | <0.1 | 0.79 | 0.046 | 90 | 400 | <0.1 |
| 6 | Fe,Cu,Al-MM(0.5/0.5)$_m$ | – | – | 0.75 | 0.048 | 90 | 330 | 39 |

[a] Reaction condition I: 1 mM PhOH, $H_2O_2$/PhOH 14/1 mol/mol, catalyst 1 g L$^{-1}$, pH 6.2, 50 °C.
[b] Reaction condition II: 10 mM PhOH, $H_2O_2$/PhOH 14/1 mol/mol, catalyst 1 g L$^{-1}$, pH 6.2, 50 °C.
[c] TOC removal was determined after 4 h of reaction.
[d] The amount of iron leached from sample to solution (based on the initial iron content in the sample).
[e] PhOH adsorption on Fe,Cu,Al-MM (100 mg) from aqueous solution (10 mM PhOH, 20 ml) after 24 h at 50 °C.
[f] ACDB adsorption on Fe,Cu,Al-MM (20 mg) from aqueous solution (0.1 mM ACDB, 20 ml) after 5 h at 50 °C.
[g] Time of 20% and 100% conversion of PhOH.

pillaring solution tends to decrease of basal spacing of Fe,Cu,Al-MMs to 15 Å that indicates the lower distortion in the clay and thus the decrease of surface area of Fe,Cu,Al-MM samples (Table 2). According to the large angle XRD result (Fig. 4), copper in Fe,Cu,Al-MMs exists as CuO, which is confirmed by the strong peaks in the region of $2\theta$ = 34.5–36.5 [46]. Note that the strong peak of $CuAl_2O_4$ at $2\theta$ = 27.7 [44] is observed in XRD pattern of Cu,Al-MM. Table 2 shows, that the texture characteristics of Fe,Cu,Al-MMs depends on the Fe/Cu ratio of pillaring solution. Generally, the average pore diameter decreases and the micropore volume increases after intercalation of clay by oligomeric Fe,Cu,Al-cations. Fe,Al-MM and Cu,Al-MM possess higher values of surface area and higher micropore content than Fe,Cu,Al-MMs.

Of special interest is the comparing of the chemical composition and textural data of Fe,Cu,Al-MM(0.5/0.5) and Fe,Cu,Al-MM(0.5/0.5)$_m$ prepared by different methods (see Section 2.2). Fe,Cu,Al-MM(0.5/0.5) has been prepared by intercalation of the natural layered aluminosilicate by mixed Fe,Cu,Al-pillaring solution (M1). Fe,Cu,Al-MM(0.5/0.5)$_m$ has been prepared by intercalation of the natural layered aluminosilicate by pillaring solution, composed of Fe,Al- and Cu,Al-solutions (M2). As Table 1 suggests, the Cu and Fe content is larger in Fe,Cu,Al-MM(0.5/0.5)$_m$ than that in Fe,Cu,Al-MM(0.5/0.5). According to DR-UV–vis spectroscopic data, the state of iron and copper in these samples depends on pillaring method (Fig. 3, spectra 2 and 6). The appearance of the strong bands at 336 and 495 nm in the spectrum of Fe,Cu,Al-MM(0.5/0.5)$_m$ indicates, that M2 promotes the formation of oligomeric species of Cu and Fe. Interestingly, textural properties of Fe,Cu,Al-MM(0.5/0.5)$_m$ agree closely with textural properties of Cu,Al-MM (Table 2). According to XRD data, the value of $d_{0\,0\,1}$ is 15 Å for Fe,Cu,Al-MM(0.5/0.5) and 18 Å for Fe,Cu,Al-MM(0.5/0.5)$_m$. This suggests that chemical composition of mixed Fe,Cu,Al-pillaring solution M1 noticeably differs from that of pillaring solution M2, composed of Fe,Al- and Cu,Al-solutions.

### 3.2. Effect of synthesis parameters on catalytic properties of Fe,Cu,Al-MMs

The results of wet phenol with $H_2O_2$ over Fe,Cu,Al-MMs at pH 6.2 are presented in Table 3. One can see catalytic activity of Fe,Al-MMs can be adjusted by Fe/Cu ratio of Fe,Cu,Al-containing pillaring solution. Notwithstanding prolonged induction period, Fe,Al-MM shows a higher activity than Cu,Al-MM analog (Fig. 5). The 100% conversion of PhOH (0.01 M solution) is reached after 300 and 530 min for Fe,Al-MM and Cu,Al-MM, correspondingly. The insertion of $Cu^{2+}$ in clay appreciably increases activity of Fe,Cu,Al-MMs and decreases induction period (Fig. 5, Table 3). It is reasonable to assume that the activity of Fe,Cu,Al-MMs is determined both by the iron species leached and the iron species present on the catalyst surface. The data of the catalytic tests in 0.01 M PhOH indicate that the catalytic activity of Fe,Cu,Al-MMs slightly depends on Fe leaching. We estimate that after iron leaching from Fe,Cu,Al-MM(0.5/0.5) the iron concentration was 1.5 mg/L in PhOH solution. In the presence of $FeCl_3$ (1.5 mg/L, pH 6.2), PhOH conversion was only 12% after 420 min. Note that without catalyst 5% of phenol was converted after 420 min. Therefore the reaction of phenol oxidation is mostly determined by the iron species present on the catalyst surface.

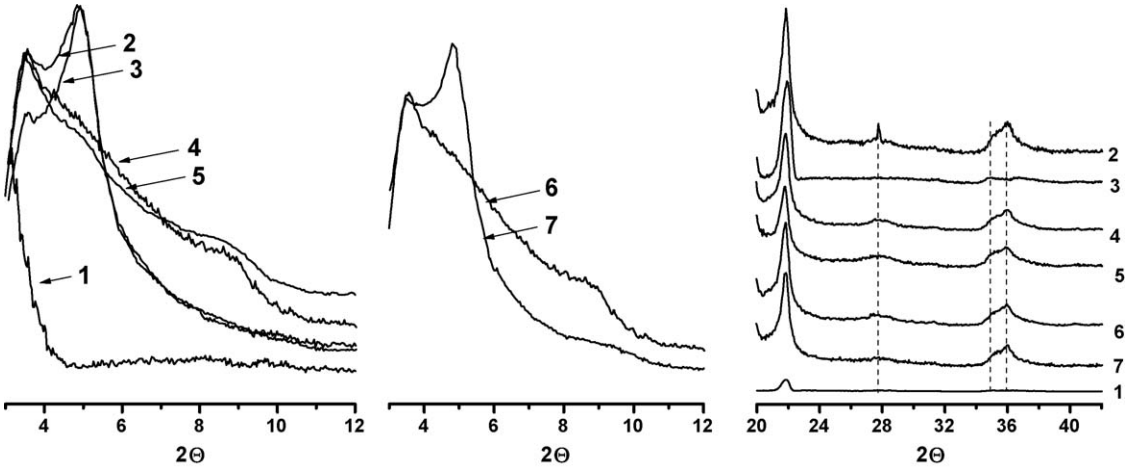


**Fig. 4.** X-ray diffraction patterns of the natural layered aluminosilicate calcined at 500°C (MM) (1), Cu,Al-MM (2), Fe,Al-MM (3), Fe,Cu,Al-MM(0.7/0.3) (4), Fe,Cu,Al-MM(0.3/0.7) (5), Fe,Cu,Al-MM(0.5/0.5) (6), Fe,Cu,Al-MM(0.5/0.5)$_m$ (7).

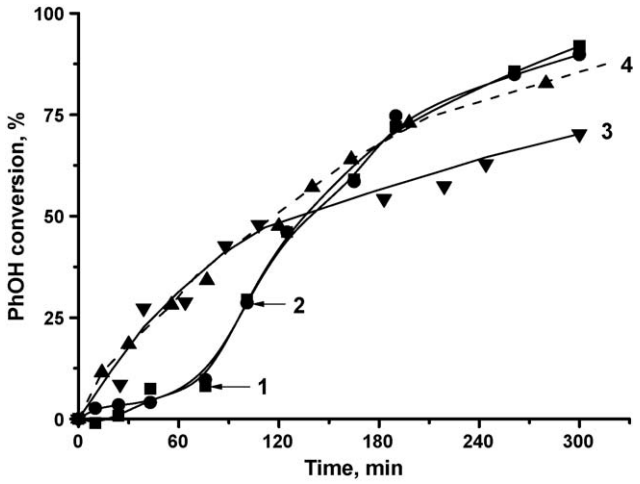


**Fig. 5.** The PhOH consumption in the presence of Fe,Cu,Al-MM(0.5/0.5)$_m$ – 1 (■), Fe,Al-MM – 2 (●), Cu,Al-MM – 3 (▼), Fe,Cu,Al-MM(0.5/0.5) – 4 (▲) (10 mM PhOH, $H_2O_2$/PhOH 14/1 mol/mol, catalyst 1 g $L^{-1}$, pH 6.2, 50 °C).

Experimental data (Table 3) clearly show that the PhOH oxidation activity relates to the iron content in Fe,Cu,Al-MMs. The time of full phenol conversion increases with the decrease of Fe content in Fe,Cu,Al-MMs: Fe,Cu,Al-MM(0.3/0.7) (10 mg/g–420 min) > Fe,Cu,Al-MM(0.5/0.5) (13 mg/g–415 min) > Fe,Cu,Al-MM(0.7/0.3) (15 mg/g–360 min). The inclusion of Cu in clay essentially decreases the induction period in comparison with Fe,Al-MM, although the catalytic activity of Fe,Cu,Al-MMs change insignificantly (Table 3, Fig. 5). The increase of reaction rate with the increase in Fe content can be explained by the increase in accessibility of Fe sites for reagents. The content of Fe sites, accessible to reagents adsorption, was evaluated by measurement of PhOH and ACDB adsorption (Table 3). The difference in adsorption values $\alpha_{PhOH}$ and $\alpha_{ACDB}$ was a direct consequence of the size and configuration of PhOH and ACDB molecules [10]. The ACDB adsorption on Fe,Cu,Al-MMs can be depictured as coordination between OH– and N=N-groups of ACDB and Fe and/or Cu ion of Fe,Cu,Al-MMs. These adsorption sites should be located in outside the interlayer space of pillared clay. The adsorption values based on specific surface area of Fe,Cu,Al-MM ($\alpha_{PhOH}$ and $\alpha_{ACDB}$) are shown in Table 3. As one can see the adsorption values for Fe,Cu,Al-MM(0.5/0.5)$_m$ and Fe,Al-MM are closely related values. At the same time the $\alpha_{ACDB}$ for Fe,Cu,Al-MMs are nearly twice as much as that for Fe,Cu,Al-MM(0.5/0.5)$_m$ and Fe,Al-MM, as a result of difference in textural properties and state of Fe and Cu in the Fe,Cu,Al-MMs (see Section 3.2).

As shown above the kinetic curve of PhOH oxidation with $H_2O_2$ over Fe,Al-MM has induction period that is typical for all Fenton like systems (Fig. 5). The inclusion of Cu in clay leads to disappearance of induction period. This phenomenon can be explained by the change in the rate of oxygen and organic radicals formation in the presence of both $Cu^{2+}$ and $Fe^{3+}$ ions. Fig. 6 shows an overview of the possible reaction pathways in the mechanisms of PhOH oxidation in the presence of heterogeneous Fe- and Cu-containing systems [19,47–49]. It is well-known that the decomposition of $H_2O_2$ by $Fe^{3+}$ goes through the formation of radical oxygen species, such as $HO_2^{\bullet}/O_2^{-\bullet}$ and $HO^{\bullet}$ radicals (Fig. 6A). $HO_2^{\bullet}/O_2^{-\bullet}$ radicals are quite unreactive compared to $HO^{\bullet}$ toward most organic substrates in aqueous solution [48]. It is generally believed that the reaction of $HO^{\bullet}$ with phenol leads to the formation of organic radicals (Fig. 6A, Eq. (7)) and the $Fe^{3+}/Fe^{2+}$ cycle is closed by reaction (5). A somewhat different mechanism of the radicals generation and phenol oxidation is proposed for Cu-containing systems [19,47]. At first stage, the $H_2O_2$ decomposition leads to the formation of hydroperoxyl radical $HO_2^{\bullet}$ and its conjugate base $O_2^{-\bullet}$ (Fig. 6B, Eq. (1)–(3)). The same of $H_2O_2$ with $Cu^{2+}$ produces $Cu^{+}$ ions and then reactive intermediate $\equiv Cu^{2+}–OH^{\bullet}$ (Eq. (1)–(2)). This intermediate attacks phenol with $PhO^{\bullet}$ radical generation (Fig. 6B,

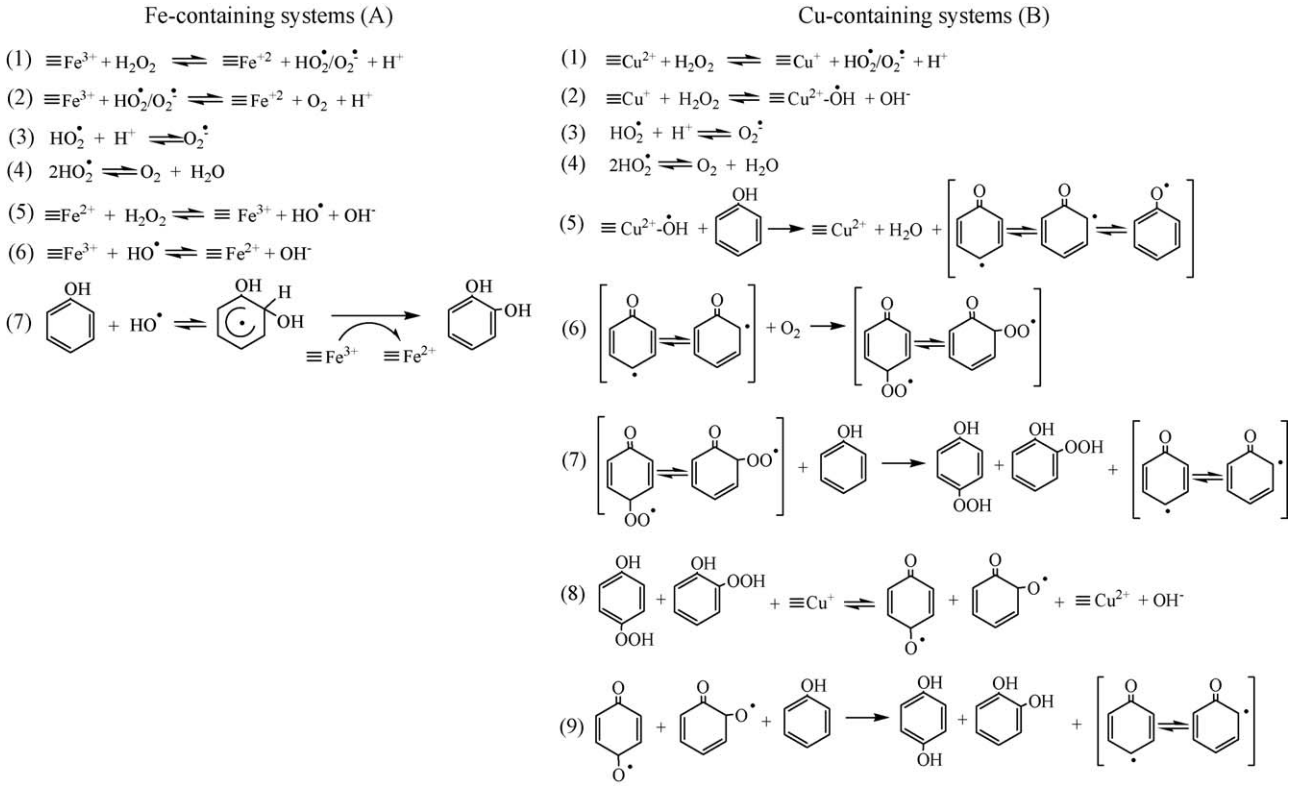


**Fig. 6.** . Mechanisms proposed for PhOH oxidation in the presence of heterogeneous Fe- and Cu-containing systems.

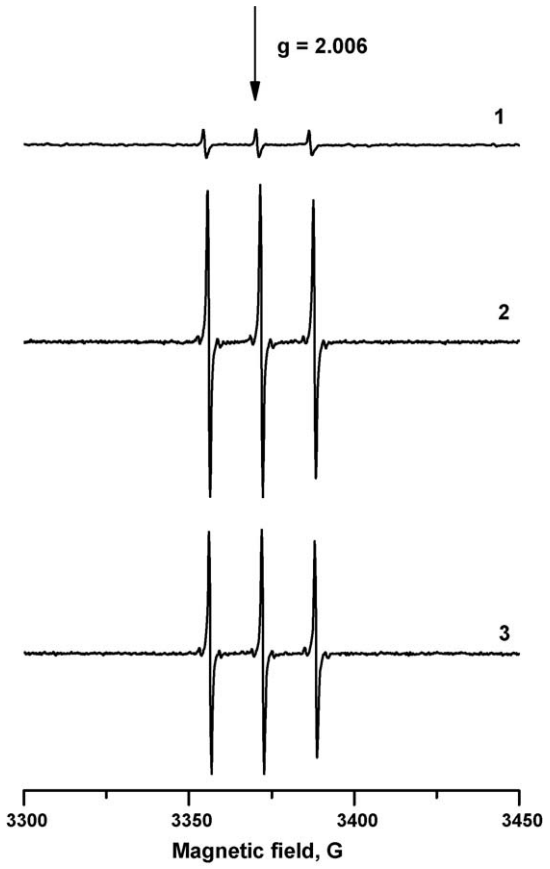


**Fig. 7.** EPR spectra of the TEMP radical adducts formed during phenol oxidation over Fe,Al-MM (1) Fe,Cu,Al-MM(0.7/0.3) (2) and Cu,Al-MM (3) (0.2 mmol PhOH, 0.58 mmol $H_2O_2$, catalyst 20 mg, 0.21 mmol TEMP, 5 ml $H_2O$, pH 5.9, 50 °C, 30 min).

Eq. (5)). The recombination of two hydroperoxyl radicals $HO_2^•$ produces molecular oxygen $O_2$ (Eq. (4)), which is likely to able to continue radical chain via formation PhO(OO)• radical (Eq. (6)). Note that molecular oxygen $O_2$ also forms in systems $Fe^{3+}$–$Fe^{2+}$/$H_2O_2$ due to reaction of $HO_2^•/O_2^{-•}$ radicals with $Fe^{3+}$ and recombination of two $HO_2^•$ radicals (Fig. 6A, Eq. (2) and (4)). The $Cu^+/Cu^{2+}$ cycle is closed by reactions (5) and (8).

Nowadays the electron spin resonance spectroscopy is common for investigation of free radical generation by the *in vivo* spin-trapping technique, when short-lived radicals are transformed into more stabilized radical scavenger adduct for EPR detection. In our work, we apply the EPR spectroscopy spin-trapping technique to probe phenol oxidation over Fe,Al-MM, Fe,Cu,Al-MM(0.7/0.3) and Cu,Al-MM using 2,2,6,6-tetramethyl-4-piperidine (TEMP) as a spin trap. TEMP was previously used for trapping of singlet molecular oxygen $O_2$ with formation of nitroxyl radical TEMPO [50]. The transformation of TEMP to TEMPO can be indirect evidence of formation of free radicals. Fig. 7 presents an EPR spectra obtained upon the addition of TEMP to the reaction solutions containing Fe,Al-MM, Fe,Cu,Al-MM(0.7/0.3) and Cu,Al-MM. The EPR signal with at $g = 2.006$ and $a^N$ 17.9 G belongs to TEMPO [51]. We compared the change of a nitroxyl radical TEMPO intensity during the reaction course with catalytic activity of Fe,Cu,Al-MM, Fe,Al-MM and Cu,Al-MM. It was found that the change of PhOH conversion during the reaction course correlates with the change of a nitroxyl radical TEMPO intensity (Fig. 8). It is reasonable to suggest that the higher catalytic activity of Fe,Cu,Al-MM(0.7/0.3), than Fe,Al-MM and Cu,Al-MM (Table 3) is result of the joint action of Cu and Fe species of Fe,Cu,Al-MM(0.7/0.3). Therefore these results clearly show that the insertion of $Cu^{2+}$ in clays appreciably increases their activity due to the change of reaction mechanisms (Fig. 6). Note that oxygen chemisorbed on the Cu-containing clay may also participate in the mechanism of oxidation of the organic species and thus, also affects the increase in its catalytic activity [19,49].

### 3.3. Fe,Cu,Al-MM stability and recycling

The phenol concentration is one of the important parameters in the stability of Fe,Cu,Al-MMs systems. As will readily be observed from Table 3, the decrease in phenol concentration favours the decrease in Fe leaching from solids. Thus, during the reaction course, the iron leaching from all Fe,Cu,Al-MM samples was <0.1 wt.% in 1 mM PhOH reaction solution. It is worth of noting that catalytic activity (TOC removal) increases with the increase of Fe content in Fe,Cu,Al-MMs (Table 3).

The data presented in Table 4 allow comparison of the catalyst stability and activity of Fe,Cu,Al-MM(0.7/0.3) and Fe,Al-MM after recycling. After each operation cycle, the catalyst was separated, washed with $H_2O$, dried, calcined at 200 °C and used in the next run. One can see that the catalytic activity of Fe,Cu,Al-MM(0.7/0.3) with respect to TOC removal decreased significantly already after the first run. At the same time the catalytic activity of Fe,Al-MM decreased after the second run. There may be several reasons for the reduction of the catalytic activity. There are changes in the state of the active site on the catalyst surface and metal ion leaching induced by the reagents and/or products. According to the DR-UV–vis spectrum of Fe,Cu,Al-MM(0.7/0.3) collected after the first catalytic cycle, the intensity of the bands at >300 nm increased, indicating that aggregated Cu and Fe are formed

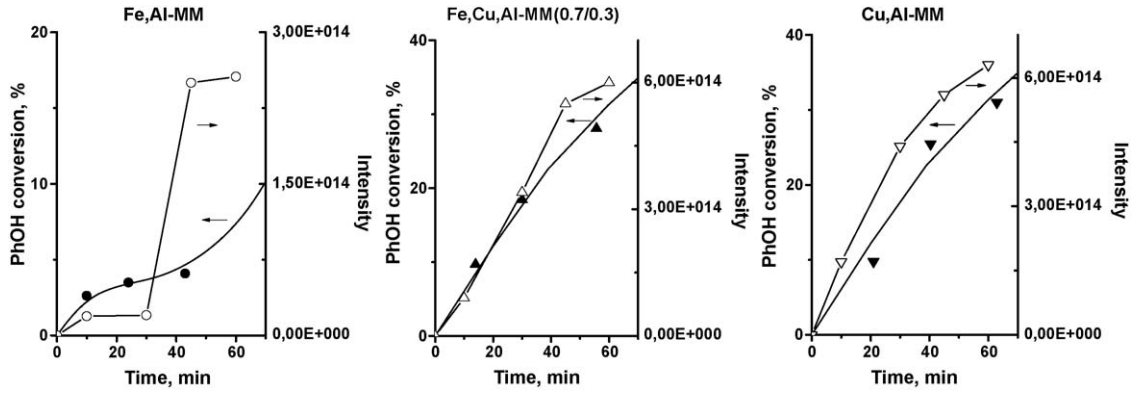


**Fig. 8.** Dependence of intensity of signals in EPR spectroscopy on the catalytic activity in phenol oxidation with $H_2O_2$ over Fe,Al-MM, Fe,Cu,Al-MM(0.7/0.3) and Cu,Al-MM (0.2 mmol PhOH, 0.58 mmol $H_2O_2$, catalyst 20 mg, 0.21 mmol TEMP, 5 ml $H_2O$, pH 5.9, 50 °C).

**Table 4**
Phenol oxidation in the presence of Fe,Cu,Al-MM samples[a].

| Sample | Run 1 | | Run 2 | | Run 3 | |
|---|---|---|---|---|---|---|
| | $\tau_{100\%}$[b] (min) | TOC removal[c] (%) | $\tau_{100\%}$[b] (min) | TOC removal[c] (%) | $\tau_{100\%}$[b] (min) | Fe leaching[d] (wt.%) |
| Fe,Cu,Al-MM(0.7/0.3) | 90 | 52 | 310 | <1 | >360 | 27 |
| Fe,Al-MM | 90 | 48 | 95 | 40 | 210 | 5 |

[a] Reaction condition: 1 mM PhOH, $H_2O_2$/PhOH 14/1 mol/mol, catalyst 1 g $L^{-1}$, pH 6.2, 50 °C
[b] Time of 40% and 100% conversion of PhOH
[c] TOC removal was determined after 4 h of reaction
[d] The amount of iron leached from sample to solution (based on the initial iron content in the sample).

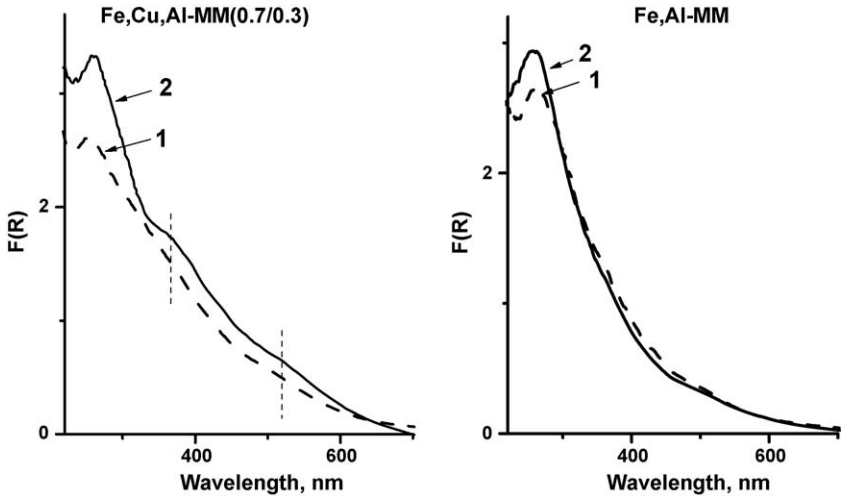


**Fig. 9.** DR-UV–vis spectra of Fe,Cu,Al-MM(0.7/0.3) and Fe,Al-MM before (1) and after the first run of PhOH oxidation (2).

(Fig. 9). This is in agreement with IR spectroscopic data. It can be seen from Fig. 10, the intensity of the band at 527 $cm^{-1}$ ($\delta$(Si–O) and $\nu$(M–O)) increases, and the bands at 882 and 855 $cm^{-1}$ can be ascribed to $\delta$(M–OH) [51] are observed in spectrum of Fe,Cu,Al-MM(0.7/0.3) after the first catalytic cycle. This means that Fe and Cu ions come out the silica–alumina framework due to the hydrolysis of M–O–Si(Al) bonds, migrate and form oligomerized $MO_x$ species on the surface. In turn, this favours leaching of iron from Fe,Cu,Al-MM(0.7/0.3) and leads to decreasing catalytic activity in second catalytic cycle of phenol oxidation (Table 4). Note that the high acidity of reaction medium due to the formation of acid intermediate products also may induce leaching of metal ions into liquid phase (Fig. 11). As one can see from Tables 3 and 4, Fe,Al-MM is more stable with respect to the iron leaching compared to Fe,Cu,Al-MMC(0.7/0.3). Thus, after three reactions cycles of PhOH oxidation iron leaching from Fe,Al-MM did occur and amounted about 5% (Table 4). In turn, the leaching of Fe atoms from Fe,Cu,Al-MM(0.7/0.3) was higher and reached 27%. The appearance of induction period in second run (Fig. 12) is evidence of copper ion leaching from Fe,Cu,Al-MM(0.7/0.3) and changes in

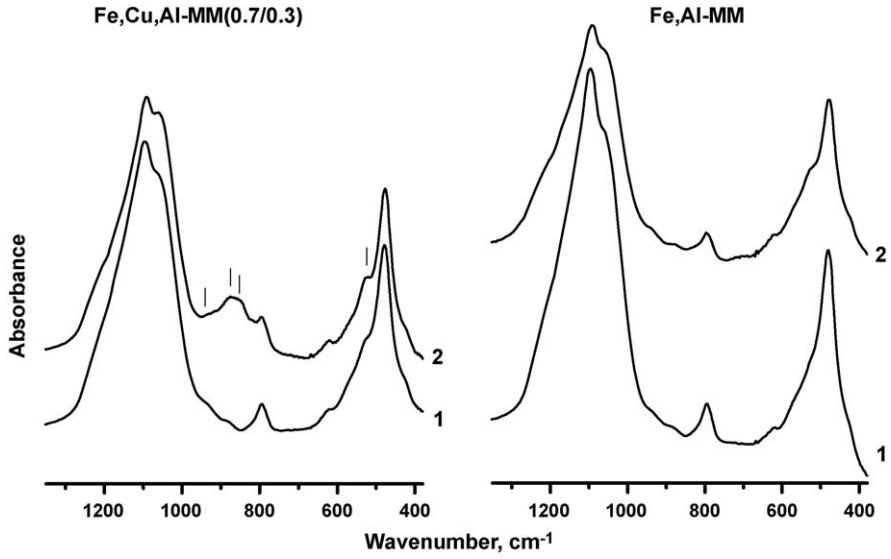


**Fig. 10.** IR spectra of Fe,Cu,Al-MM(0.7/0.3) and Fe,Al-MM before (1) and after the first run of PhOH oxidation (2).

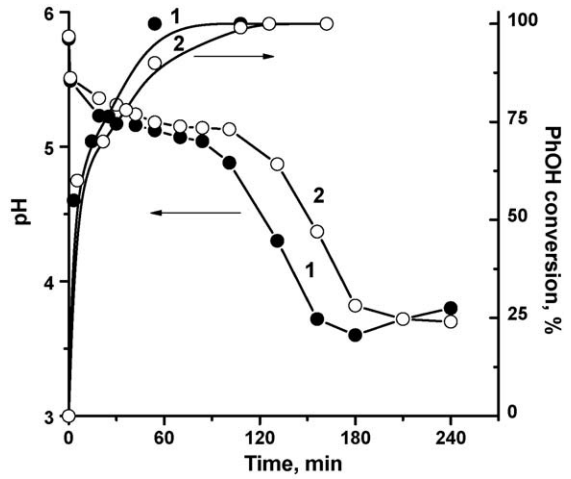


**Fig. 11.** The phenol consumption and changes in pH of solution in phenol oxidation over Fe,Cu,Al-MM(0.3/0.7) – 1 (●) and Fe,Cu,Al-MM(0.7/0.3) – 2 (○) (catalyst 1.0 g $L^{-1}$, PhOH 1 mM, $H_2O_2$ 14 mM, pH = 6.2, 50 °C).

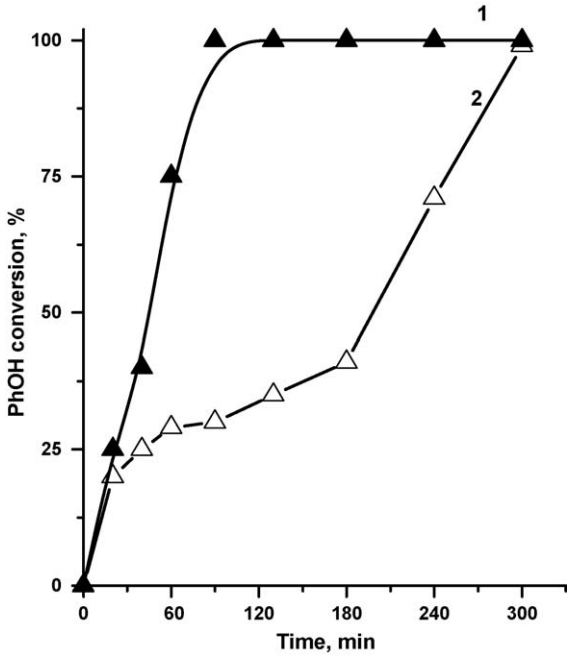


**Fig. 12.** The phenol consumption in phenol oxidation over fresh Fe,Cu,Al-MM(0.7/0.3) (1) and Fe,Cu,Al-MM(0.7/0.3) used after the first run (2).

the state of the active site on the catalyst surface. Therefore, we may conclude that the insertion of copper ions in clay favours the increase in catalytic activity, but negative affects the stability of Fe,Cu,Al-MM systems.

## 4. Conclusion

The mixed Fe,Cu,Al-containing clays (Fe,Cu,Al-MM) have been synthesized from natural layered aluminosilicate by exchanging interlayer ions to polyoxocations. The nature of polyoxocations was varied by using (a) partially hydrolyzed Fe,Cu,Al-containing pillaring solutions (M1); and (b) mixture of two partially hydrolyzed Fe/Al and Cu/Al pillaring solutions (M2). It has been shown that textural properties of Fe,Cu,Al-containing clays can be controlled by Fe/Cu ratio of Fe,Cu,Al-containing pillaring solution and nature of polyoxocation. The increase in copper loading leads to the decrease in total surface area, micropore volume and interlay distance of Fe,Cu,Al-MMs. The insertion of Cu in the natural layered aluminosilicate favours the formation of iron oligomer and/or aggregated iron oxide clusters. Fe,Al-MM possesses the larger amount of extra framework than Fe,Cu,Al-MMs.

Fe,Cu,Al-MMs were tested as catalysts for wet phenol oxidation with $H_2O_2$. The insertion of Cu in pillared clay decreases the induction period and increases the catalytic activity of Fe,Cu,Al-MMs. Fe,Cu,Al-MM prepared by method M1 was more effective catalytic system than system prepared by method M2, because method M2 promotes the formation of oligomeric species of Cu and Fe. The formation of the great amount of aggregated iron and copper oxide clusters favours the increase of iron leaching from Fe,Cu,Al-MM(M2). The content of Fe sites, i.e. accessible sites to reagents adsorption, was evaluated by measurement of PhOH and ACDB adsorption. It was found, that the adsorption values for Fe,Cu,Al-MMs are nearly twice as much as that for Fe,Cu,Al-MM(M2) and Fe,Al-MM, that is a result of difference in textural properties and state of Fe and Cu in the Fe,Cu,Al-MMs.

The insertion of copper ions in clay favours the increase in catalytic activity of Fe,Cu,Al-MMs due to the joint action of Cu and Fe species towards increasing radical generation.

## Acknowledgement

This work was supported by Russian Foundation for Basic Research under Grant 07-90100-a, 06-08-01064-a and 08-08-00729-a. We thank Dr. Yu.A. Chesalov for IR measurements.

## References

[1] G. Centi, S. Perathoner, Microporous Mesoporous Mater. 107 (2008) 3.
[2] A. Gil, S.A. Korili, M.A. Vicente, Catal. Rev. Sci. Eng. 50 (2008) 153.
[3] G. Centi, S. Perathoner, T. Torre, M.G. Verduna, Catal. Today 55 (2000) 61.
[4] A. Gil, L.M. Gandia, M.A. Vicente, Catal. Rev. Sci. Eng. 42 (1–2) (2000) 145.
[5] I. Palinko, A. Molnar, J.B. Nage, J.C. Bertrand, K. Lazar, J. Valyon, I. Kiricsi, J. Chem. Soc., Faraday Trans. 3 (1997) 1591.
[6] D. Zhao, G. Wang, Y. Yang, X. Guo, Q. Wang, J. Ren, Clays Clay Miner. 41 (1993) 317.
[7] J. Barrault, C. Bouchoule, J.-M. Tatibouët, M. Abdellaoui, A. Majesté, I. Louloudi, N. Papayannakos, N.H. Gangas, Stud. Surf. Sci. Catal. 130 (2000) 749.
[8] I. Kiricsi, A. Molnar, I. Palinko, K. Lazar, Stud. Surf. Sci. Catal. 94 (1995) 63.
[9] M.N. Timofeeva, S.C. Khankhasaeva, S.V. Badmaeva, A.L. Chuvilin, E.B. Burgina, A.B. Ayupov, V.N. Panchenko, A.V. Kulikova, Appl. Catal. B: Environ. 59 (2005) 243.
[10] M.N. Timofeeva, S.Ts. Khankhasaeva, Yu.A. Chesalov, S.V. Tsybulya, V.N. Panchenko, E.Ts. Dashinamzhilova, Appl. Catal. B: Environ. 88 (1–2) (2009) 127–134.
[11] A. Gil, A. Diaz, M. Montes, D.R. Acosta, J. Mater. Sci. 29 (1994) 4927.
[12] Y.S. Shin, S.G. Oh, B.H. Ha, Korean J. Chem. Eng. 20 (1) (2003) 77.
[13] W.O. Parker Jr., I. Kiricsi, Appl. Catal. A: Gen. 121 (1995) L7.
[14] H.Y. Zhu, E.F. Vansant, J.A. Xia, G.Q. Lu, J. Porous Mater. 4 (1997) 17.
[15] L.M. Gandı, M.A. Vicente, P. Oelker, P. Grange, A. Gil, React. Kinet. Catal. Lett. 64 (1998) 145.
[16] C. Flego, L. Galasso, R. Millini, I. Kiricsi, Appl. Catal. A: Gen. 168 (1998) 323.
[17] J. Carriazo, E. Gue.lou, J. Barrault, J.M. Tatibouet, R. Molina, S. Moreno, Catal. Today 126 (2005) 107–108.
[18] M. Kurian, S. Sugunan, Chem. Eng. J. 115 (2006) 139.
[19] S. Caudo, G. Centi, C. Genovese, S. Perathoner, Top. Catal. 40 (1–4) (2006) 207.
[20] N. Frini, M. Crespin, M. Trabelsi, D. Messad, H. Van Damme, F. Bergaya, Appl. Clay Sci. 12 (3) (1997) 281.
[21] J.G. Carriazo, E. Guelou, J. Barrault, J.M. Tatibouët, S. Moreno, Appl. Clay Sci. 22 (6) (2003) 303.
[22] J. Barrault, C. Bouchoule, K. Echachoui, N. Frini-Srasra, M. Trabelsi, F. Bergayn, Appl. Catal. B: Environ. 15 (1998) 269.
[23] H. Pérez-Vidal, E. Custodio-García, E. López-Alejandro, J. Morales-Hidalgo, D.M. Frías-Márquez, Sol. Energy Mater. Sol. Cells 90 (6) (2006) 841.
[24] R. Ben Achma, A. Ghorbel, S. Sayadi, A. Dafinov, F. Medina, J. Phys. Chem. Solids 69 (5–6) (2008) 1116.
[25] S.C. Kim, D.K. Lee, Catal. Today 97 (2004) 153.
[26] A. Schutz, W.E.E. Stone, G. Pongelet, J.J. Fripiat, Clay Clay Miner. 35 (1987) 251.
[27] T.J. Pinnavaia, M.S. Tzou, S.D.L. Landau, R.H. Raythatha, J. Mol. Catal. 27 (1984) 195.
[28] M. Akitt, N.N. Greenwood, B.L. Khandelwal, G.D. Laster, J. Chem. Soc., Dalton Trans. 5 (1972) 604.
[29] C. Feng, H. Tang, D. Wang, Colloids Surf. A: Physicochem. Eng. Aspects 305 (2007) 76.
[30] P. Wu, T. Komatsu, T. Yashima, Microporous Mesoporous Mater. 20 (1998) 13.
[31] G.J. Kim, W.S. Ahn, Zeolites 11 (1991) 745.
[32] V.C. Farmer, The Infrared Spectra of Minerals, Mineral Soc., London, 1974.
[33] C. Mosser, L.J. Michot, F. Villieras, M. Romeo, Clays Clay Miner. 45 (1997) 789.

[34] J.T. Kloprogge, E. Mahmutagic, R.L. Frost, J. Colloid. Interface Sci. 296 (2006) 640.
[35] J. Madejova, Vib. Spectro. 31 (2003) 1.
[36] D.M. Sherman, Phys. Chem. Minerals 12 (1985) 161.
[37] Y. Li, Zh. Feng, Y. Lian, K. Sun, L. Zhang, G. Jia, Q. Yang, C. Li, Microporous Mesoporous Mater. 84 (2005) 4.
[38] B. Montanari, A. Vaccari, M. Gazzano, P. Kabner, H. Papp, J. Pasel, R. Dziembaj, W. Makowski, T. Lojewski, Appl. Catal. B Environ. 13 (1997) 205.
[39] Y. Teraoka, C. Tai, H. Ogawa, H. Furukawa, S. Kagawa, Appl. Catal. A 200 (2000) 167.
[40] Y. Wang, Q. Zhang, T. Shishido, K. Takehira, J. Catal. 209 (2002) 186.
[41] S.E. Dapurkar, S.K. Badamali, P. Selvam, Catal. Today 68 (2001) 63.
[42] H. Praliaud, S. Mikhailenko, Z. Chajar, M. Primet, Appl. Catal. B Environ. 16 (1998) 359.
[43] M.C.N.A. de Carvalho, F.B. Passos, M. Schmal, Appl. Catal. A 193 (2000) 265.
[44] J. Levec, Appl. Catal. 63 (1990) Ll10.
[45] L. Bergaoui, J.-M. Lamert, H. Suquet, M. Che, J. Phys. Chem. 99 (1995) 2155.
[46] Q. Wu, X. Hu, P.L. Yue, X.S. Zhao, G.Q. Lu, Appl. Catal. B: Environ. 32 (2001) 151.
[47] G. Fu, L.F. Nazar, A.D. Bain, Chem. Mater. 3 (1991) 602.
[48] J. Pignatello, E. Oliveros, A. MacKay, Crit. Rev. Environ. Sci. Technol. 36 (2006) 1.
[49] A. Santos, P. Yustos, A. Quintanilla, F. Garcia-Ochoa, Top. Catal. 33 (1–4) (2005) 181.
[50] T. Wu, J. Shen, A. Song, S. Chen, M. Zhang, T. Shen, J. Photochem. Photobiol. B: Biol. 57 (2000) 14.
[51] G.K. Kustova, E.B. Burgina, V.A. Sadykov, S.G. Poryvaev, Phys. Chem. Miner. 18 (1992) 379.